

MATHEMATICAL MODELLING OF MULTI-PHASE FLOW USING ENTROPY SYMMETRIZATION

P. Cordesse^{1,2}, M. Massot², A. Murrone¹

¹ ONERA

Chemin de la Hunière 91123 Palaiseau, FRANCE
pierre.cordesse@polytechnique.edu, angelo.murrone@onera.fr

² CMAP

Route de Saclay 91128 Palaiseau Cedex, FRANCE
marc.massot@polytechnique.edu

Key words: Multiphase flow, entropy symmetrization, numerical simulation

Abstract. Jet atomizations play a crucial role in many applications such as in cryogenic combustion chambers. Since direct numerical simulations of these two-phase flows in engine real configurations are still out of reach, predictive numerical tools must be developed using reduced-order models with sound mathematics properties. The contribution of this paper is three-fold. First, we introduce a new formalism to symmetrize non-conservative systems using entropic variables by extending Mock-Godunov theory and apply it to the Baer-Nunziato model. This new theory broaches new leads to obtain an original Eulerian diffuse interface model describing various mixture disequilibrium level based on an a consolidated mixture thermodynamic. Second, to cope with the strong discontinuities encountered in jet atomization, a robust and accurate numerical method using multi-slope MUSCL technique is applied to the various levels of the diffuse interface models. Third, relying on the previous two points, simulations of a jet atomization in a cryogenic combustion chamber in subcritical conditions are presented using diffuse interface models with thermal and velocity disequilibria coupled to an Eulerian kinetic-based moment method.

1 Introduction

Jet atomizations play a crucial role in many industrial applications such as in cryogenic combustion chambers. The multi-scale and various physical phenomena occurring embrace high level of complexity and the strong interaction of the latter is a current research area. In particular, the stability and the efficiency of the engine are extremely correlated to the way the liquid oxygen is injected and its primary atomization. It may also lead to high frequencies instabilities which could severely damage the rocket, thus must be thoroughly studied. Experimentations are conducted to enable simulation validation and

to understand the observed physical phenomena, but are very costly and restricted in the range of operating points. Therefore predictive numerical simulations are mandatory, at least as a complementary tool to understand the physic and even more to conceive new combustion chambers and predict instabilities they may generate in a given configuration. Focusing on a LOX GH2 cryogenic combustion chamber in a subcritical regime, a complex two-phase flow takes place between the liquid oxygen and the gaseous hydrogen injected at the rear center of the chamber through a coaxial injector. Near the injector, the two phases are separated by a clean interface until high shear stress tears the liquid core into ligaments which eventually collapse into a spray of droplets. Thus a transition zone between the *separated phase zone* and the *dispersed phase zone*, denoted the *mixed region*, involves very complex subscale physics and topologies of the flow. Direct numerical simulations (DNS) could be used to resolve this elaborate flow and would offer in theory a full resolution of the interface. Still DNS in a real configuration of a engine are still out of reach, CPU needs being too high and defining the smallest scale of a two-phase mixture is still unclear. Thus, predictive numerical tools must be developed through reduced-order models. Attention must be paid on the mathematics properties and the predictiveness of such reduced-order models. In the literature, two main strategies are encountered to build them. (1) *coupled models* up to three, one adapted for each phase topology. In the *separated phase zone*, two approach are found: either two-fluid models derived by diffuse-interface methods or by front tracking method. The former uses a statistical averaging of the instantaneous Navier-Stokes equations for each phase [3]. The latter includes some level of space filtering as done by [13]. As for the *dispersed phase zone*, the particles are tracked either in a Lagrangian way [22], or by an Eulerian approach where the droplets distribution is rebuilt thanks to the method of moments [21]. Usually, the methods applied to the *separated phase zone* are extended to *the mixed region*, but it implies either a high level of the phase disequilibrium description or a extremely refined mesh. (2) the complexity of interfacing several models has pushed towards deriving a *unified model* coping all the flow regimes as proposed recently in [4] where some sub-scale phenomena are accounted for in the *separated and mixed regions* and degenerate into a predictive spray model in the disperse flow area [6] [5]. In this work, the first approach has been chosen by coupling a diffuse interface method to a member of the kinetic based moment methods (KBMM). In [16], the homogeneous two-phase flow model, referred as the *four-equation model*, has been used for the two first regimes. However to describe accurately *the mixed region* and to provide enough informations to feed the polydispersity of the spray offered by the KBBM candidate, all level of phase disequilibrium must be kept, that is to say, each phase must have its own pressure, velocity and pressure. Consequently, the Baer-Nunziato model [1], called the *seven-equation model* (*7eq. model*), appears as the best candidate. Extended by the work of [18] thanks to the introduction of interfacial quantities, the model writes:

$$\partial_t \mathbf{u} + A_1 \partial_x \mathbf{u} = \frac{\mathbf{R}(\mathbf{u})}{\epsilon} \text{ with } A_1 = \partial_{\mathbf{u}} \mathbf{f}(\mathbf{u}) + \mathbb{G}(\mathbf{u}) = \begin{pmatrix} u_I & 0 & 0 \\ \mathbf{g}_2(\mathbf{u}_2) & \partial_{\mathbf{u}_2} \mathbf{f}(\mathbf{u}_2) & 0 \\ \mathbf{g}_1(\mathbf{u}_1) & 0 & \partial_{\mathbf{u}_1} \mathbf{f}(\mathbf{u}_1) \end{pmatrix} \quad (1)$$

where the quasi conservative variables are $\mathbf{u} = (\alpha_2, \mathbf{u}_2, \mathbf{u}_1)^t$, $\mathbf{u}_k = (\alpha_k \rho_k, \alpha_k \rho_k u_k, \alpha_k \rho_k E_k)$, the conservative fluxes $\mathbf{f}(\mathbf{u}) = (\alpha_k \rho_k u_k, \alpha_k \rho_k u_k^2 + \alpha_k p_k, \alpha_k (\rho_k E_k + p_k) u_k)^t$. \mathbb{G} is the matrix containing the non-conservative terms $\mathbf{g}_2(\mathbf{u}_2) = -\mathbf{g}_1(\mathbf{u}_1) = (0, p_I, p_I u_I)^t$, α_k is the volume fraction of phase $k = 1, 2$, ρ_k the partial density, u_k the phase velocity, p_k the phase pressure, $E_k = \epsilon_k + 1/2 u_k^2$ the total energy per unit of mass, ϵ_k the internal energy associated usually to a two-parameter equation of state, u_I the interfacial velocity and p_I the interfacial pressure, both to be modelled. The two phases can not stay in full disequilibrium, \mathbf{R} is thus an application describing usually the mechanical and hydrodynamic relaxations between the two phases and is designed by physical processes respecting the entropy inequality. It decomposes classically onto

$$\frac{\mathbf{R}}{\epsilon} = \frac{\mathbf{R}^u}{\epsilon_u} + \frac{\mathbf{R}^p}{\epsilon_p}, \text{ with } \frac{\mathbf{R}^u}{\epsilon_u} = \left(0, \frac{\mathbf{R}_2^u}{\epsilon_u}, \frac{\mathbf{R}_1^u}{\epsilon_u}\right)^t \text{ and } \frac{\mathbf{R}^p}{\epsilon_p} = \left(\frac{p_2 - p_1}{\epsilon_p}, \frac{\mathbf{R}_2^p}{\epsilon_p}, \frac{\mathbf{R}_1^p}{\epsilon_p}\right)^t \quad (2)$$

where ϵ reads as the characteristic time for each of these processes, $\mathbf{R}_2^u = -\mathbf{R}_1^u = (0, u_2 - u_1, u_I(u_2 - u_1))$, $\mathbf{R}_2^p = -\mathbf{R}_1^p = (0, 0, p_I(p_2 - p_1))$. The mathematical properties of the *7eq. model* have been studied in [9] among others. It is hyperbolic, admits seven eigenvalues $(u_I, (u_k, u_k \pm a_k)_{k=2,1})$ with a_k the phase sound of speed, $a_k^2 = \partial p_k / \partial \rho_k|_{s_k}$. Nonetheless the model is strictly hyperbolic only under the *non resonance condition* [2]. The interfacial terms u_I and p_I modelling varies but usually, to facilitate numerical implementation, conditions have been sought to make $\lambda_1 = u_I$ linearly degenerate. Assuming first that the interfacial velocity u_I has a symmetric form $u_I = \beta u_1 + (1 - \beta) u_2$, then β has no choice but to be defined as $\beta \in \{0, 1, \alpha_1 \rho_1 / \rho\}$ where ρ is the mixture density $\rho = \alpha_1 \rho_1 + \alpha_2 \rho_2$. An expression for the relaxation parameters ϵ_u and ϵ_p have been for example derived using the DEM technique in [19]. From this *7eq. model*, a hierarchy of two-phase flow models can be obtained: the instantaneous relaxation of the pressures and the velocities leads to the *five-equation model* [14]. When relaxing instantaneously the temperatures through as supplementary relaxing term, one obtains the compressible Navier-Stokes equations, called also *four-equation model*. This hierarchy of diffuse interface model is very appealing. The *7eq. model* offers a state of full-disequilibrium as long as adequate relaxing times are used for the relaxation processes. In cryogenic applications, the pressure of the phases may be considered relaxed instantaneously. However, due to the strong velocity and temperature gradients at the interface, it is unrealistic to assume hydrodynamic and thermal instantaneous relaxation. Simulations including a temperature disequilibrium have already been conducted on real configurations, but it seems it has never been done with also a velocity disequilibrium [20]. The reason lies in the difficulty of first defining a momentum interfacial transfer subgrid model and second in designing robust numerical methods able to cope a non slip velocity. Therefore, we would like in the first section to deepen the mathematical study of the *7eq. model* to better understand its structure focusing on the relaxation terms. Currently, the latter have been postulated by physical interpretations and shaped using the entropy inequality. It means there expression relies on the choice of the entropy and thus on the thermodynamic of a mixture. So far, the mixture entropy \mathbf{H} being widely used leads to the decoupling of the relaxing phenomena in order to close the model. We propose to symmetrize for the first

time the hyperbolic Baer-Nunziato model using generalized entropic variables as done for multi-species Eulerian systems in [17]. It will help to generate general relaxation source terms compatible with the entropy inequality. In the next section, numerical methods applied to the coupled models are described emphasizing the relaxation procedure. Finally, results of numerical simulations are reported ahead of future perspectives.

2 Symmetrization of a non-conservative system using entropic variables

This section recalls first the theory of entropy symmetrization of conservative systems developed by Mock and Godunov [12]. We then propose a novel extension of this theory to non-conservative hyperbolic systems (Equation (3)) and apply it on the *7eq. model*.

$$\partial_t \mathbf{u} + \{\partial_u \mathbf{f}(\mathbf{u}) + \mathbb{G}(\mathbf{u})\} \partial_x \mathbf{u} = \mathbf{R}(\mathbf{u})/\epsilon \quad (3)$$

2.1 Mock-Godunov's theorem for conservative systems

Mock-Godunov's theorem stipulates that a conservative hyperbolic Equation (3) ($\mathbb{G}(\mathbf{u}) = 0$) may have a symmetric form thanks to a variable change if it has a generalized strictly convex entropy \mathbf{H} with the corresponding fluxes \mathbf{G} [12]. The entropy equation writes:

$$\textit{Entropy equation} \quad \partial_t \mathbf{H} + \partial_u \mathbf{G}(\mathbf{u}) \partial_x \mathbf{u} = 0 \quad (4)$$

The change variable is then \mathbf{v} defined by $\mathbf{v} = \partial_u \mathbf{H}^t$ [10]. Taking the scalar product of Equation (3) ($\mathbb{G}(\mathbf{u}) = 0$) and \mathbf{v} raises the following compatibility equations:

$$\textit{Compatibility equations} \quad \partial_{uu} \mathbf{H} \cdot \partial_u \mathbf{f}(\mathbf{u}) = \partial_u \mathbf{G}(\mathbf{u}) \text{ and } \mathbf{v} \cdot \mathbf{R}(\mathbf{u})/\epsilon \leq 0 \quad (5)$$

Deriving Equation (5) LHS leads to a symmetric condition on the conservative terms:

$$\partial_{uu} \mathbf{H} \cdot \partial_u \mathbf{f}(\mathbf{u}) + \partial_u \mathbf{H} \cdot \partial_{uu} \mathbf{f}(\mathbf{u}) = \partial_{uu} \mathbf{G}(\mathbf{u}) \quad (6)$$

Theorem 1. [11] $\partial_{uu} \mathbf{H} \cdot \partial_u \mathbf{f}(\mathbf{u})$ is symmetric if and only if there is an entropy flux \mathbf{G} associated with the entropy \mathbf{H} .

Finally, assuming that the mapping $\mathbf{u} \rightarrow \mathbf{v}$ is diffeomorph, the quasi linear system using generalized entropic variables writes:

$$\tilde{A}_0 \partial_t \mathbf{v} + \tilde{A}_1 \partial_x \mathbf{v} = \mathbf{R}/\epsilon \quad (7)$$

where $\tilde{A}_0 = \partial_v \mathbf{u} = (\partial_{uu} \mathbf{H})^{-1}$ and $\tilde{A}_1 = A_1 \times \tilde{A}_0 = \partial_u \mathbf{f}(\mathbf{u}) \cdot (\partial_{uu} \mathbf{H})^{-1}$. Therefore, to symmetrize a hyperbolic conservative system in the sens of Mock-Godunov, only one supplementary condition to the Theorem 1 is necessary.

Theorem 2. [11] *Given an hyperbolic conservative system, if one of the following conditions holds:*

(C₁) $\partial_{uu} \mathbf{H} \cdot \partial_u \mathbf{f}(\mathbf{u})$ is symmetric

(C₂) there is an entropy flux \mathbf{G} associated with the entropy \mathbf{H}

then, the symmetrized form in the sens of Mock-Godunov of the hyperbolic conservative system can be derived if and only if the following condition holds:

(S₁) $\partial_{uu} \mathbf{H}$ is invertible $\Leftrightarrow \mathbf{H}$ strictly convex

2.2 Extension to non-conservative hyperbolic systems

A non-conservative hyperbolic Equation (3) may have a symmetric form thanks to a variable change if it has a generalized strictly convex entropy \mathbf{H} with the corresponding entropy flux \mathbf{G} such that the entropy equation writes:

$$\textit{Extended entropy equation} \quad \partial_t \mathbf{H} + \partial_{\mathbf{u}} \mathbf{G}(\mathbf{u}) \partial_x \mathbf{u} = \mathbf{R}(\mathbf{u})/\epsilon \quad (8)$$

Assuming such entropy flux \mathbf{G} exists, keeping the same change variable $V = \partial_{\mathbf{u}} \mathbf{H}^t$, its scalar product with Equation (3) LHS raises the following extended compatibility equations:

$$\partial_{\mathbf{u}} \mathbf{H}^t \cdot \{\partial_{\mathbf{u}} \mathbf{f}(\mathbf{u}) + \mathbb{G}(\mathbf{u})\} = \partial_{\mathbf{u}} \mathbf{G}(\mathbf{u}) \text{ and } \mathbf{v} \cdot \mathbf{R}(\mathbf{u})/\epsilon \leq 0 \quad (9)$$

The Jacobian of the entropy flux vector, $\partial_{\mathbf{u}} \mathbf{G}$, is then decomposed into two components, \mathbf{a} and \mathbf{b} , which both contribute to the conservative fluxes \mathbf{f} and the non-conservative terms \mathbb{G} , the latter ones being hence decomposed into $\partial_{\mathbf{u}} \mathbf{f} = \mathbb{M}_1 + \mathbb{N}_1$ and $\mathbb{G} = \mathbb{M}_2 + \mathbb{N}_2$. $\partial_{\mathbf{u}} \mathbf{G}(\mathbf{u})$ is thus finally decomposed into $\partial_{\mathbf{u}} \mathbf{G}(\mathbf{u}) = \mathbf{a}_1 + \mathbf{a}_2 + \mathbf{b}_1 + \mathbf{b}_2$ to obtain the following set of equations and conditions:

$$\left\{ \begin{array}{l} \partial_{\mathbf{u}} \mathbf{H} \cdot \mathbb{M}_k = \mathbf{a}_k, \quad \partial_{\mathbf{u}} \mathbf{H} \cdot \mathbb{N}_k = \mathbf{b}_k \\ \partial_{\mathbf{u}} \mathbf{H} \cdot \partial_{\mathbf{u}} \mathbf{f} = \mathbf{a}_1 + \mathbf{b}_1 \\ \partial_{\mathbf{u}} \mathbf{H} \cdot \mathbb{G} = \mathbf{a}_2 + \mathbf{b}_2 \end{array} \right. \quad \text{with the conditions} \quad \left\{ \begin{array}{l} \partial_{\mathbf{u}} (\mathbf{a}_1 + \mathbf{a}_2) \text{ symmetric} \\ \mathbf{b}_1 + \mathbf{b}_2 = 0 \\ \partial_{\mathbf{u}} \mathbf{H}^t \cdot \mathbf{R}(\mathbf{u})/\epsilon \leq 0 \end{array} \right. \quad (10)$$

The condition on \mathbf{b} implies that $\partial_{\mathbf{u}} \mathbf{G}(\mathbf{u}) = \mathbf{a}_1 + \mathbf{a}_2$. This condition has been chosen due to the fact that the scalar $\mathbf{b}(\mathbf{u}) \partial_x \mathbf{u}$ will not be signable since it is a non-conservative term and a constant dilatation of time and space ($t \rightarrow \lambda t$, $x \rightarrow \lambda x$) would change it. Applying Equation (10) to Equation (8) defines an extended compatibility equation with respect to Equation (5):

$$\textit{Extended Compatibility Equation} \quad \partial_{\mathbf{u}} \mathbf{H}^t \cdot [\mathbb{M}_1 + \mathbb{M}_2] = \mathbf{a}_1 + \mathbf{a}_2 \quad (11)$$

and differentiating it, one obtains a new equation imposing symmetry conditions just as for the conservative systems:

$$\partial_{\mathbf{u}\mathbf{u}} \mathbf{H} \cdot [\mathbb{M}_1 + \mathbb{M}_2] + \partial_{\mathbf{u}} \mathbf{H} \cdot \partial_{\mathbf{u}} [\mathbb{M}_1 + \mathbb{M}_2] = \partial_{\mathbf{u}} (\mathbf{a}_1 + \mathbf{a}_2) = \partial_{\mathbf{u}\mathbf{u}} \mathbf{G}(\mathbf{u}) \quad (12)$$

Theorem 3. $\partial_{\mathbf{u}\mathbf{u}} \mathbf{H} \cdot [\mathbb{M}_1 + \mathbb{M}_2] + \partial_{\mathbf{u}} \mathbf{H} \cdot \partial_{\mathbf{u}} [\mathbb{M}_1 + \mathbb{M}_2]$ is symmetric if and only if there is an entropy flux \mathbf{G} associated with the entropy \mathbf{H}

Proof. See proof of Theorem 1 □

Finally, the quasi linear system using generalized entropic variables writes:

$$\tilde{A}_0 \partial_t \mathbf{v} + \tilde{A}_1 \partial_x \mathbf{v} = \mathbf{R}/\epsilon \quad (13)$$

where $\tilde{A}_0 = (\partial_{\mathbf{u}\mathbf{u}} \mathbf{H})^{-1}$ and $\tilde{A}_1 = [\partial_{\mathbf{u}} \mathbf{f}(\mathbf{u}) + \mathbb{G}(\mathbf{u})] \cdot (\partial_{\mathbf{u}\mathbf{u}} \mathbf{H})^{-1}$. Therefore, to symmetrize a hyperbolic conservative system in the sens of Mock-Godunov, only two supplementary conditions to the Theorem 3 are necessary.

Theorem 4. *Given an hyperbolic conservative system, if one of the following conditions holds:*

(C₁) $\partial_{\mathbf{u}\mathbf{u}}\mathbf{H} \cdot [\mathbb{M}_1 + \mathbb{M}_2] + \partial_{\mathbf{u}}\mathbf{H} \cdot \partial_{\mathbf{u}}(\mathbb{M}_1 + \mathbb{M}_2)$ *is symmetric*

(C₂) *there is an entropy flux \mathbf{G} associated with the entropy \mathbf{H}*

then, the symmetrized form in the sens of Mock-Godunov of the hyperbolic conservative system can be derived if and only if the two following conditions hold:

(S₁) $\partial_{\mathbf{u}\mathbf{u}}\mathbf{H}$ *is invertible* $\Leftrightarrow \mathbf{H}$ *strictly convex*

(S₂) $\partial_{\mathbf{u}\mathbf{u}}\mathbf{H} \cdot [\mathbb{M}_1 + \mathbb{M}_2 + \mathbb{N}_1 + \mathbb{N}_2]$ *must be symmetric* $\Leftrightarrow \partial_{\mathbf{u}}\mathbf{H} \cdot \partial_{\mathbf{u}}[\mathbb{M}_1 + \mathbb{M}_2 + \mathbb{N}_1 + \mathbb{N}_2]$ *must be symmetric*

Proof. (S₁) see proof in Theorem 2. For (S₂)

$$\begin{aligned} & \partial_{\mathbf{u}\mathbf{u}}\mathbf{H} \cdot [\partial_{\mathbf{u}}\mathbf{f}(\mathbf{u}) + \mathbb{G}(\mathbf{u})] \text{ must be symmetric to have } \tilde{A}_1 \text{ symmetric} \\ \implies & \partial_{\mathbf{u}\mathbf{u}}\mathbf{H} \cdot [\mathbb{M}_1 + \mathbb{M}_2] + \partial_{\mathbf{u}\mathbf{u}}[\mathbb{N}_1 + \mathbb{N}_2] \text{ symmetric} \\ \implies & \underbrace{\partial_{\mathbf{u}\mathbf{u}}\mathbf{G}(\mathbf{u})}_{\text{symmetric}} - \partial_{\mathbf{u}}\mathbf{H} \cdot \partial_{\mathbf{u}}[\mathbb{M}_1 + \mathbb{M}_2] + \partial_{\mathbf{u}}\left(\underbrace{\partial_{\mathbf{u}}\mathbf{H} \cdot \partial_{\mathbf{u}}[\mathbb{N}_1 + \mathbb{N}_2]}_{=0 \text{ condition on } \mathbf{b}}\right) - \partial_{\mathbf{u}}\mathbf{H} \cdot \partial_{\mathbf{u}}[\mathbb{N}_1 + \mathbb{N}_2] \text{ symmetric} \\ \implies & \partial_{\mathbf{u}}\mathbf{H} \cdot \partial_{\mathbf{u}}[\mathbb{M}_1 + \mathbb{M}_2 + \mathbb{N}_1 + \mathbb{N}_2] \text{ symmetric} \end{aligned}$$

□

2.3 Application to the Baer-Nunziato system

In the Baer-Nunziato model (Equation (1)), by expressing the entropic variables as $\mathbf{v} = (V_\alpha, \mathbf{v}_2, \mathbf{v}_1)^t$ and \mathbf{a}_k and \mathbf{b}_k (line vectors) as $\mathbf{a}_k = (a_k^\alpha, \mathbf{a}_k^2, \mathbf{a}_k^1)$, $\mathbf{b}_k = (b_k^\alpha, \mathbf{b}_k^2, \mathbf{b}_k^1)$, the Equation (10) reads:

$$\begin{aligned} 0 &= a_1^\alpha + b_1^\alpha & V_\alpha u_I + \mathbf{v}_2 \cdot \mathbf{g}_2 + \mathbf{v}_1 \cdot \mathbf{g}_1 &= a_2^\alpha + b_2^\alpha \\ \mathbf{v}_2^t \cdot \partial_{\mathbf{u}_2}\mathbf{f}(\mathbf{u}_2) &= \mathbf{a}_1^2 + \mathbf{b}_1^2 & 0 &= \mathbf{a}_2^2 + \mathbf{b}_2^2 \\ \mathbf{v}_1^t \cdot \partial_{\mathbf{u}_1}\mathbf{f}(\mathbf{u}_1) &= \mathbf{a}_1^1 + \mathbf{b}_1^1 & 0 &= \mathbf{a}_2^1 + \mathbf{b}_2^1 \end{aligned} \quad (14)$$

with the conditions $\partial_{\mathbf{u}}(\mathbf{a}_1 + \mathbf{a}_2)$ symmetric and $\mathbf{b}_1 + \mathbf{b}_2 = 0$. The classic mixture entropy proposed for this model is defined as $\mathbf{H} = -\sum_{k=1,2} \alpha_k \rho_k s_k$, with s_k the phase entropy, and there exists an associated entropy flux \mathbf{G} defined by $\mathbf{G} = -\sum_{k=1,2} \alpha_k \rho_k s_k u_k$. The generalized entropic variables \mathbf{v} are $\mathbf{v} = (v_\alpha, \mathbf{v}_2^t, \mathbf{v}_1^t)^t$ with $V_\alpha = p_1/T_1 - p_2/T_2$, $\mathbf{v}_k = ((g_k - 1/2u_k^2)/T_k, u_k/T_k, -1/T_k)^t$, $k = 1, 2$ and g_k is the Gibbs free energy, $g_k = \epsilon_k + p_k/\rho_k - T_k s_k$. Interestingly, two compatible choices for the decomposition of the Jacobian of the entropic flux $\partial_{\mathbf{u}}\mathbf{G}$ appear:

$$\mathbf{a}_1 = \begin{pmatrix} Y \\ \mathbf{v}_2^t \cdot \partial_{\mathbf{u}_2}\mathbf{f}(\mathbf{u}_2) \\ \mathbf{v}_1^t \cdot \partial_{\mathbf{u}_1}\mathbf{f}(\mathbf{u}_1) \end{pmatrix} \mathbf{b}_1 = \begin{pmatrix} -Y \\ 0 \\ 0 \end{pmatrix} \mathbf{a}_2 = \begin{pmatrix} Z \\ 0 \\ 0 \end{pmatrix} \mathbf{b}_2 = \begin{pmatrix} -Z + v_\alpha u_I \sum_{k=1,2} \mathbf{v}_k \cdot \mathbf{g}_k \\ 0 \\ 0 \end{pmatrix} \quad (15)$$

with either $(Y, Z) = (\Gamma, 0)$ or $(Y, Z) = (0, \Gamma)$ where $\Gamma = p_1 u_1/T_1 - p_2 u_2/T_2$. Corresponding decomposition of \mathbf{f} and \mathbf{G} is not unique. For $\kappa = \frac{p_1 u_1/T_1 - p_2 u_2/T_2}{p_1/T_1 - p_2/T_2}$, possible choices are

$$\mathbb{M}_1 = \begin{pmatrix} X & 0 & 0 \\ 0 & \partial_{\mathbf{u}_2}\mathbf{f}(\mathbf{u}_2) & 0 \\ 0 & 0 & \partial_{\mathbf{u}_1}\mathbf{f}(\mathbf{u}_1) \end{pmatrix} \mathbb{N}_1 = \begin{pmatrix} -X & 0 & 0 \\ 0 & 0 & 0 \\ 0 & 0 & 0 \end{pmatrix} \mathbb{M}_2 = \begin{pmatrix} 0 & 0 & 0 \\ \mathbf{j}_2 & 0 & 0 \\ \mathbf{j}_1 & 0 & 0 \end{pmatrix} \mathbb{N}_2 = \begin{pmatrix} u_I & 0 & 0 \\ g_2 - \mathbf{j}_2 & 0 & 0 \\ g_1 - \mathbf{j}_1 & 0 & 0 \end{pmatrix} \quad (16)$$

with either $(X, \mathbf{j}_k) = (\kappa, \mathbf{0})$ or $(X, \mathbf{j}_k) = (0, \boldsymbol{\chi}_k)$ respectively to Equation (15) where $\boldsymbol{\chi}_k = (0, (-1)^k p_k, 0)^t$ or $\boldsymbol{\chi}_k = (0, 0, (-1)^k p_k u_k)^t$. It is important to notice that Theorem 2 and 4 depend only on \mathbf{a} and \mathbf{b} or equivalently on the sum of the matrix $\mathbb{M}_1, \mathbb{N}_1, \mathbb{M}_2, \mathbb{N}_2$. Hence, for each decomposition above, the condition on $(\mathbf{b}_1 + \mathbf{b}_2)$ writes: $\sum_{k=1,2} \frac{1}{T_k} (p_k - p_I) (u_I - u_k) \partial_x \alpha_k = 0$. A unique solution on p_I satisfies this condition and is $p_I = \mu p_1 + (1 - \mu) p_2$, with $\mu(\beta) = [(1 - \beta) T_2] / [\beta T_1 + (1 - \beta) T_2]$. Simple calculations show that $\partial_{\mathbf{u}}(\mathbf{a}_1 + \mathbf{a}_2)$ is indeed symmetric in each case. However, first $\partial_{\mathbf{u}\mathbf{u}}\mathbf{H} = \partial_{\mathbf{u}}\mathbf{v}^t$ is not invertible since $\det(\partial_{\mathbf{u}\mathbf{u}}\mathbf{H}) = 0$. \mathbf{H} is indeed not strictly convex. Second, the symmetry conditions of Theorem 4 are not verified. Therefore it is not possible to derive a symmetrized form in the sens of Mock-Godunov of the system with the classic mixture entropy. The underlying reason leading to a non strictly convex mixture entropy is the assumed thermodynamic of the mixture. Indeed, defining \mathbf{H} the classic way means a mixture acts as if each phase does not see one another, there is no interaction on their thermodynamic which is defined by a two-parameters equation of state $s_k = s_k(\rho_k, \epsilon_k)$. In [1], the phase entropy s_k is found to depend also on the volume fraction α_k accounting for the compaction of the granular bed. In [9] a mathematical mixture entropy \mathcal{H} is given as $\mathcal{H} = -\sum_{k=1,2} \alpha_k \rho_k [\ln(s_k(\rho_k, p_k)) + \psi_k(\alpha_k)]$ without justifying its definition and without using it. We are currently investigating a new consistent mixture thermodynamic which raises a strictly convex mixture entropy and could then lead to a symmetrized form of the *7eq. model*.

3 Numerical methods

The models used hereafter to simulate the jet atomization have been implemented in the CEDRE software which is a multi-physics platform working on general unstructured meshes and organized as a set of solver [8]. Two solvers are used, *SEQUOIA* for the diffuse interface model and *SPIREE* for the KBMM. Since the work on the extended thermodynamic of a mixture is not yet completely validated, the present diffuse interface model applied in the *separated-phase and mixed regions* is the classical euler *7eq. model* defined in Equation (1). As our primary concern is to increase the disequilibrium in the interface diffuse model, for sake of simplicity, a simple KBMM element has been chosen for the *dispersed phase region*: a multi-fluid modelling with sampling methods [15] along with a monokinetic and monothermal assumption of the droplet size distribution. Evaporation and coalescence of the droplets are neglected, thus only one sample of droplet is needed to attest the success of the coupling strategy of the two models. The two models are two-way coupled through the source terms $S_{q \rightarrow u}$ and $S_{u \rightarrow q}$ which model the atomization of the liquid phase into droplets and the pseudo-coalescence of the droplets into the liquid phase but also through S_{drag} the drag force of the gas acting upon the droplets and S_h the conducto-convective heat transfer at the surface of the droplet. A Lie splitting technique is used resulting in the following system:

$$\mathbf{U}^{n+1} = \left[S_{u \rightarrow q} - S_h - S_{drag} \frac{\mathbf{R}^u}{\epsilon_u} \right]^{\Delta t} \frac{\mathbf{R}^p}{\epsilon_p} \mathcal{H}_u(\mathbf{U}^n) \quad \mathbf{Q}^{n+1} = [S_{q \rightarrow u} S_h S_{drag}]^{\Delta t} \mathcal{H}_q(\mathbf{U}^n) \quad (17)$$

The hyperbolic operators \mathcal{H}_u and \mathcal{H}_q , of the two-fluid model and the dispersed model respectively, are calculated using an approximate Riemann solver, HLLC, and an Pressureless Gas Dynamics exact Riemann solver respectively. Then relaxation operators and source terms are applied in the order showed in System (17) to define the new states \mathbf{U}^{n+1} and \mathbf{Q}^{n+1} of the conservative variables. For the *7eq. model*, to ensure good robustness of the scheme, a MUSCL-Hancock strategy with a multi-slope MUSCL spatial reconstruction scheme has been applied [7]. Strong assumptions are made to tackle certain issues by assuming (1) the interfacial terms p_I and u_I to be local constants in the Riemann problem, (2) the volume fraction to vary only across the interfacial contact discontinuity u_I . As a result, the non conservative terms in System (1) vanish, u_I and p_I are determined locally by Discrete Equation Method (DEM) [19] at each time step and stay constant during the update. Thus, phases are now decoupled and the system (1) splits into two conservative sub-systems to which a classic HLLC solver is implemented. Finally, a hybrid limiter has been used to combines the advantages of a CFL-Superbee limiter for high gradient regions and a third order CFL dependent limiter for the regular regions [16].

3.1 Relaxation procedure

In many applications, the pressures of a two-phase flow are assumed to relax instantaneously. Thus, after the hyperbolic update, the following ODE is solved: $\partial_t \mathbf{U} = \mathbf{R}^p(\mathbf{U})/\epsilon_p$, with $\epsilon_p \rightarrow \infty$ which infers u_k remain constant. Manipulating the equations, an equilibrium pressure is obtained by solving a second order equation with an iterative procedure such as a Newton method [7]. As for the velocities, within the context of jet atomization in subcritical conditions, the relaxation time is in theory finite. The following ODE is solved: $\partial_t \mathbf{U} = \mathbf{R}^u(\mathbf{U})/\epsilon_u$ which implies α_k, ρ_k are conserved during the relaxation. Subtraction of the momentum equations gives the following ODE on the split velocity $u_d = u_2 - u_1$: $\partial_t u_d - A^o u_d / \epsilon_u = 0$. A first numerical approach is to fix a remaining slip velocity ratio target at each time step Δt . It defines the characteristic relaxing time $\epsilon_u / A^o = \ln(X) \Delta t$ with $X = u_d^{\Delta t} / u_d^o$ and $A^o = (\alpha_1^o \rho_1^o + \alpha_2^o \rho_2^o) / (\alpha_1^o \rho_1^o \alpha_2^o \rho_2^o)$. An instantaneous velocity relaxation is in practice also possible and leads to a unique relaxed velocity which is the mass weighted average of the two velocities before relaxing.

3.2 Coupling source terms

The physical processes accounted for in the coupling source terms are the atomization of the liquid phase, S_{atom} , and the pseudo-coalescence of the liquid droplets, S_{coal} . They are defined as follows: $S_{atom} = \alpha_2 \rho_2 f_{atom} \lambda_{atom}$ and $S_{coal} = \alpha_d \rho_d f_{coal} \lambda_{coal}$ where f_{atom} is the atomization frequency, λ_{atom} describes the efficiency of the atomization, f_{coal} the pseudo-coalescence frequency and λ_{coal} the pseudo-coalescence efficiency, defined all in [16]. Thanks to the increase of disequilibrium by using the *7eq. model* with finite velocity relaxation, S_{atom} has been revisited making full use of the existence of two velocities to track regions with high shear stress and thus regions where atomization should occur.

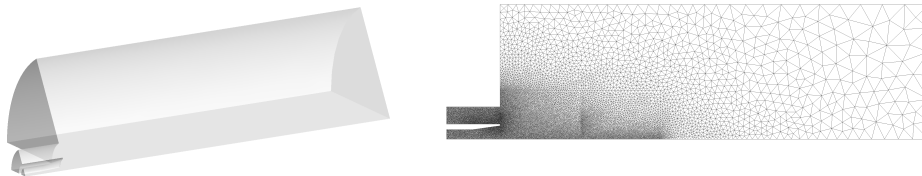
4 Results and Discussion

From the hierarchy of diffuse interface model have been retained the *instantaneously relaxed 7eq. model (IR7eq)* and the *non-instantaneously relaxed 7eq. model (NIR7eq)* to perform numerical simulations. Their prime purpose is to validate the numerical method robustness when allowing velocity disequilibrium and model coupling. The impact on the liquid core length, its dynamics, the sharpness of the interface and the velocities at the interface is then evaluated. The operation conditions being so close to a real configuration, the results may also be predictive.

4.1 Description of the configuration

The configuration choice meets several criteria mimicking the experimental test-bench MASCOTTE, a cryogenic rocket engine combustion chamber. Adopting a unique coaxial injector of liquid oxygen O_2 (l) circumscribed by gaseous hydrogen H_2 (g), it offers a portion $\theta \in [0, \pi/3]$ of a cylindrical chamber to capture the dynamic of the jet. As a result, the computational time is thus not too heavy to conduct numerical tests and validations but the liquid jet will not flap. Mesh refinement has been applied in the region of the

Figure 1: Geometry and mesh of the configuration (around a million cells)



injector to capture the interface dynamics (see Figure 1). The injector lip of length L^{lip} is meshed by four cells at the minimum mesh size Δx_{min} . Walls are set to adiabatic slip boundaries, the variables $(\rho_k, u_k, T_k, \alpha_k)$ define the inlets, the outlet is pressure defined at $p_\infty = 10 \text{ bar}$. The momentum ratio $J = \rho_1 u_1^2 / (\rho_2 u_2^2) \sim 3$, temperature ratio $T_1/T_2 \sim 3$ and the residual phase volume fraction $\epsilon_\alpha = 1e^{-6}$. The numerical simulation has been conducted as followed: first, the oxygen and the hydrogen have been injected with a ramp-up to reach at $\tau = \tau_0$ the operating point using the *five-equation model* with no coupling. Then, the simulation has run approximately ten times the characteristic convective time of the liquid core τ_{conv} . At this point designated by τ_1 has started the comparison of the models.


4.2 Comparison of the models

For the first time, we have successfully conducted a simulation of jet atomization with an atomized *NIR7eq*. The simulation has run for $2.5\tau_{\text{conv}}$ attesting the success of the implementation. Figure 2 presents the volume fraction of liquid droplets α_d and the norm

Figure 2: atomized *NIR7eq* (Legend: blue isovolume of $\alpha_2 = 0.99$, slip velocity norm $|\mathbf{u}_{slip}|$, volume fraction of droplets in the SPIREE solver α_d)



of the slip velocity in the two-phase flow $|\mathbf{u}_{slip}|$. The slip velocity is highly concentrated in the interface region, on the so-to-say "gaseous side", where atomization occurs. It permits to give to the atomized liquid droplets the speed of the liquid phase. It is a major gain of accuracy as long as the characteristic time of velocity relaxation is physically well-defined. At the present time, the characteristic time is finite and constant, but it will be reviewed in future works to match the physical reality. Then, Figure 3 shows qualitatively the liquid interface after $1.5\tau_{conv}$ simulation time and compare it to the *IR7eq*. The latter is not coupled with atomization since S_{atom} needs a non zero slip velocity. Interestingly,

Figure 3: Comparison of the liquid volume fraction α_2 : slice at $\theta=\pi/6$, at $T=T_1$ (left) and $T=T_1+1.5\tau_{conv}$ (right), $\alpha_2=1.0$  $\alpha_2=0.01$

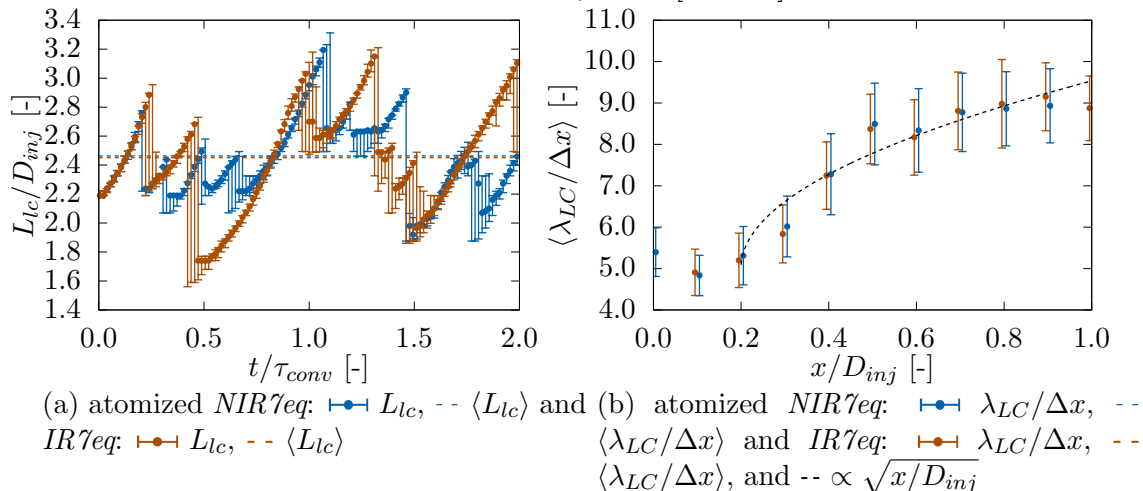


the liquid core is very similar for the two models meaning the atomization process is not interfering with the liquid core. Moreover a quantification of the liquid core length and the interface diffusion for the two models is proposed hereafter. The length of the liquid core L_{lc} varies over time witnessing the pulsation of the jet. The two models behave similarly and show the same time averaged length (Figure 4a). Figure 4b quantifies the interface diffusion close to the injection which overlaps from 5 to 9 mesh cells. Distinction must be made between numerical diffusion and physical diffusion. The numerical diffusion of a discontinuity is proportional to the square root of its travelled distance whereas physical diffusion may be due to folding of the interface which cannot be captured by the mesh. Figure 4b seems to capture numerical diffusion mainly. Applied further down the liquid core, this analysis could help us to detect where a sub-grid model would be needed to capture correctly physical processes such as ligaments detaching or interface folding.

5 Conclusion

This paper has presented first an extension of the symmetrization theory of Mock-Godunov for non-conservative systems. It has permitted to reinterpret the classic Baer Nunziato model but has shown the limit of the classic mixture thermodynamic. Then, for the first time, numerical simulation in quasi real configuration has been conducted with a *NIR7eq* model coupled to a simple KBMM element. The numerical implementation has shown

Figure 4: Comparison of the liquid core length L_{lc} over time at isovalue $\alpha_2 = 0.95 \pm 0.04$ and of the interface diffusion λ_{LC} defined by $\alpha_2 \in [0.1, 0.9]$



to be robust enough to cope with the strong gradients in velocity and temperature. Atomization has been successfully implemented and fed with the liquid velocity. Results have shown that atomization and velocity disequilibrium do not interfere with the liquid core dynamics and its shape. Future works include the extension of the mixture thermodynamic and the symmetrization of the γ eq. model, a physical dynamic definition of the velocity characteristic relaxation time. This study has been co-funded by the French Aerospace Lab ONERA and the French Space Agency CNES.

References

- [1] Baer, M. R. and Nunziato, J. W., A two-phase mixture theory for the Deflagration-to-Detonation Transition (DDT) in reactive granular materials. *Int. J. Multiphase Flow* (1986) **12**:6:861–889.
- [2] Coquel, F., Hérard, J.-M., Saleh, K., and Seguin, N., Two properties of two-velocity two-pressure models for two-phase flows. *Commun. Math. Sci.* (2014) **12**:593–600.
- [3] Drew, D., Mathematical Modeling of Two-Phase Flow. *Annu. Rev. Fluid Mech.* (1983) **15**:291–291.
- [4] Drui, F. “Eulerian modeling and simulations of separated and disperse two-phase flows : development of a unified modeling approach and associated numerical methods for highly parallel computations”. PhD Thesis. Université Paris-Saclay, July 2017.
- [5] Essadki, M., De Chaisemartin, S., Laurent, F., and Massot, M. “High order moment model for polydisperse evaporating sprays towards interfacial geometry description”. in revision to SIAP. 2018.
- [6] Essadki, M., De Chaisemartin, S., Massot, M., Laurent, F., Larat, A., and Jay, S., Adaptive Mesh Refinement and High Order Geometrical Moment Method for the

- Simulation of Polydisperse Evaporating Sprays. *Oil & Gas Science and Technologie, Rev. IFP Energies nouvelles* (2016) **71**:5:25.
- [7] Furfaro, D. and Saurel, R., A simple HLLC-type Riemann solver for compressible non-equilibrium two-phase flows. *Computers & Fluids* (2015) **111**:159–178.
- [8] Gaillard, P., Le Touze, C., Matuszewski, L., and Murrone, A., Numerical Simulation of Cryogenic Injection in Rocket Engine Combustion Chambers. *AerospaceLab* (2016) 11:16.
- [9] Gallouët, T., Hérard, J.-M., and Seguin, N., Numerical modeling of two-phase flows using the two-fluid two-pressure approach. *Math. Models Methods Appl. Sci.* (2004) **14**:05:663–700.
- [10] Giovangigli, V. and Massot, M., Asymptotic Stability of equilibrium states for multicomponent reactive flows. *Math. Methods Appl. Sci.* (1998) **8**:2:251–297.
- [11] Godlewski, E. and Raviart, P.-A. *Numerical Approximation of Hyperbolic Systems of Conservation Laws*. Springer 1996.
- [12] Harten, A. and Hyman, J. M., Self adjusting grid methods for one-dimensional hyperbolic conservation laws. *J. Comput. Phys.* (1983) **50**:2:235–269.
- [13] Hecht, N. “Large eddy simulation for liquid-gas flow : application to atomization”. PhD Thesis. INSA de Rouen, Mar. 2016.
- [14] Kapila, A. K., Menikoff, R., Bdzil, J. B., Son, S. F., and Stewart, D. S., Two-phase modeling of deflagration-to-detonation transition in granular materials: Reduced equations. *Phys. Fluids* (2001) **13**:10:3002–3024.
- [15] Laurent, F. and Massot, M., Multi-fluid modelling of laminar polydisperse spray flames: origin, assumptions and comparison of sectional and sampling methods. *Combust. Theor. Model.* (2001) **5**:4:537–572.
- [16] Le Touze, C. “Coupling between separated and dispersed two-phase flow models for the simulation of primary atomization in cryogenic combustion”. PhD Thesis. Université Nice Sophia Antipolis, 2015.
- [17] Magin, T., Graille, B., and Massot, M., Thermo-chemical dynamics and chemical quasi-equilibrium of plasmas in thermal non-equilibrium. *Ann. Research Briefs, CTR, Stanford Uni.* (2009).
- [18] Saurel, R. and Abgrall, R., A Multiphase Godunov Method for Compressible Multifluid and Multiphase Flows. *J. Comput. Phys.* (1999) **150**:2:435–467.
- [19] Saurel, R., Gavriluk, S., and Renaud, F., A multiphase model with internal degrees of freedom : application to shock-bubble interaction. *J. Fluid Mech.* (2003) **495**:283–321.
- [20] Saurel, R. and Pantano, C., Diffuse-Interface Capturing Methods for Compressible Two-Phase Flows. *Annu. Rev. Fluid Mech.* (2018) **50**:1:105–130.
- [21] Sibra, A., Dupays, J., Murrone, A., Laurent, F., and Massot, M., Simulation of reactive polydisperse sprays strongly coupled to unsteady flows in solid rocket motors: Efficient strategy using Eulerian Multi-Fluid methods. *J. Comput. Phys.* (2017) **339**:210–246.
- [22] Zamansky, R., Coletti, F., Massot, M., and Mani, A., Turbulent thermal convection driven by heated inertial particles. *J. Fluid Mech.* (2016) **809**:390–437.